PROGRESS IN COLOR, COLORANTS AND COATINGS

available online @ www.pccc.icrc.ac.ir

Progress in Color Colorants Coating 16 (2023), 387-398

Ministry of Science, Research and Technology
Institute for Color Science & Technology

Investigation of Equilibrium, Isotherm, and Mechanism for the Efficient Removal of 3-Nitroaniline Dye from Wastewater Using Mesoporous Material MCM-48

A. E. Mahdi[1], N. S. Ali[2], K. R. Kalash[3], I. K. Salih[4], M. A. Abdulrahman[1], T. M. Albayati*[1]

[1.] Department of Chemical Engineering, University of Technology-Iraq, P.O. Box: 35010, Baghdad, Iraq.

[2.] Materials Engineering Department, College of Engineering, Mustansiriyah University, P.O. Box: 1000, Baghdad, Iraq.

[3.] Environment and Water Directorate, Ministry of Science and Technology, Baghdad, Iraq.

[4.] Department of Chemical Engineering and Petroleum Industries, Al-Mustaqbal University College, P.O. Box: 51001, Babylon, Iraq.

ARTICLE INFO

Article history:
Received: 06 March 2023
Final Revised: 08 June 2023
Accepted: 10June 2023
Available online: 10 Sep 2023

Keywords:
3-Nitrobenzenamine
Adsorption kinetics;
Adsorption thermodynamic
Wastewater treatment
Adsorption mechanism

ABSTRACT

In this work, the MCM-48 mesoporous material was prepared and characterized to apply it as an active adsorbent for the adsorption of 3-Nitroaniline (3-Nitrobenzenamine) from wastewater. The MCM-48 characterizations were specified by implementing various techniques such as; scanning electron microscopy (SEM), Energy dispersive X-Ray analysis (EDAX), X-ray diffraction (XRD), Brunauer-Emmett-Teller (BET) surface area, pore size distribution (PSD), and Fourier transform infrared (FTIR). The batch adsorption results showed that the MCM-48 was very active for the 3-Nitroaniline adsorption from wastewater. The adsorption equilibrium results were analyzed by applying isotherms like Langmuir and Freundlich. The maximum experimental uptake of 3-Nitroaniline according to type I Langmuir adsorption was found to be 89 mg g^{-1} approximately. The Langmuir model is superior to the Freundlich model for the adsorption of 3-Nitroaniline onto the mesoporous material MCM-48. The results demonstrated that 3-Nitroaniline regression coefficients are so high (0.99), the pseudo 2nd order hypothesis for the adsorption mechanism process appears to be well-supported. The findings of adsorption isotherms and kinetics studies indicate the adsorption mechanism is a chemisorption and physical adsorption process. In a thermodynamic analysis, a spontaneous and exothermic adsorption has been observed. Prog. Color Colorants Coat. 16 (2023), 387-398© Institute for Color Science and Technology.

1. Introduction

Wastewater produced by manufacturing locations can be treated in sewage treatment stations. The majority of industrial operations, including chemical and petrochemical plants, petroleum refineries, and chemical plants, have their own unique facilities to handle their effluent water [1]. The non-volatile stable substance 3-nitroaniline ($C_6H_6N_2O_2$), also referred to as meta-nitroaniline and m-nitroaniline, is frequently used as a dyeing agent. An aniline with a nitro functional group in position 3 is known as a 3-nitroaniline. It is described as "not easily compostable" and having "low bioaccumulation potential" and is stable in neutral, acidic, or alkaline conditions. It is used as a chemical intermediate for azo coupling component 17 and the dyes disperse yellow 5 and acid blue 29. The chemical is changed to other substances (dyestuffs and *m*-nitrophenol) during the dyeing process and application

*Corresponding author: * Talib.M.Naieff@uotechnology.edu.iq
Doi: 10.30509/pccc.2023.167111.1205

of natural dyes along with nanoparticles to finding definite properties [2-4]. Many serious environmental problems were caused by wastewater containing 3-nitroaniline, because of its carcinogenic properties and high toxicity. Present technologies for a stream of wastewater remediation and recycling also include technology of membrane encompassing reverse ultra-filtration (UF), microfiltration (MF), and osmosis) RO) [5-8]. Membrane systems have alternatives, such as chemically based oxidation processes and air/oxygen-based on non or oxidation. The first class comprises advanced oxidation processes (AOPs), which produce hydroxyl radicals that are then used for oxidation by using hydrogen peroxide, UV light, and ozone [9-12]. The second class consists of wet air, catalytic wet air, and dry oxidation [13-15]. Another type of treatment used in wastewater cleanup is adsorption. Adsorption techniques have been used to eliminate organic and inorganic contaminants from wastewater, with a particular emphasis on the usage of various materials as the preferred adsorbent. It may be said that the regeneration of the used adsorbent materials is a time-consuming and expensive procedure [13]. Because of this, there is interest in creating new adsorbents to remove contamination in the aqueous waste stream [14, 15]. Based on the size, shape, and other characteristics of a molecule, such as polarity, Zeolites can reject or selectively adsorb certain compounds. This means that they can act as adsorbents. Organ clays have been the focus of several investigations on organic molecule adsorption from aqueous solutions. There have been reports on silicate [16], mesoporous materials [17], modified and unmodified zeolites [18]. For application in separation procedures as an adsorbent, the candidate MCM-48 appears to be more promising. Scientists have been very interested in the mesoporous material such as MCM-41, MCM-48, and SBA-15 because of its potential use as supports of catalyst, catalysts, drug delivery, and absorbents [19, 20]. These material properties are high thermal stability, specific pore volume up to 1.2 cm^3g^{-1}, surface areas (1000-1500 m^2g^{-1}), a narrow pore-size distribution, and ‘‘non-cytotoxic’’ properties [21]. Mesoporous silica-based materials, including MCM-48, have been developed as efficient catalyst carriers, adsorbents, and cutting-edge drug delivery systems. [22]. This is due to their very considerable thermal stabilities, porous morphologies, extremely large surface areas, and highly reactive surfaces for the presence of the silanol groups [23, 24].

The main aim of the present research was to investigate the removal of 3-Nitroaniline ($C_6H_6N_2O_2$) from wastewater solutions by applying MCM-48 as an efficient adsorbent. The adsorption isotherms, kinetics, and thermodynamic were examined. Moreover, the adsorption mechanism of 3-Nitroaniline wastewater onto the surface of MCM-48 adsorbent was studied in a batch adsorption process. Finally, regeneration and desorption kinetics were also tested for MCM-48 to discover the actual adsorbent utility and its applicability for reusability in a continuous adsorption system. To our knowledge, no publishing results is recommending on the investigation of 3-Nitroaniline (3-Nitrobenzenamine) removal from aqueous solution by MCM-48 adsorbent. It is acquiring special recognition and considers as a promising alternative to conventional water treatment in textile industries.

2. Experimental

2.1. Chemicals

The chemicals applied for this work were cetyl trimethyl ammonium bromide $C_{19}H_{42}BrN$ (CTAB; purity >98%) as a surfactant, tetraethyl orthosilicate $Si(OC_2H_5)_4$ (TEOS; purity > 98 % (as a silica source, sodium hydroxide (NaOH), hydrochloric acid (HCl), and 3-Nitroaniline (3-Nitrobenzenamine) ($C_6H_6N_2O_2$). All reactants were analytically purchased from Sigma Aldrich Chemical Company. All materials were applied without additional purification.

2.2. Preparation of MCM-48

According to the preparation method outlined by [25-27], MCM–48 was synthesized. The following steps were used to create MCM-48 in a representative preparation: 90 g of deionized water mixed with 10 g of CTAB. 1 g of NaOH was then mixed with the solution after it had been rapidly agitated at 35 °C for 40 minutes. Eleven cm^3 of TEOS was added, after stirring the solution for 60 minutes at 35 °C, and the mixture was then stirred at this temperature for another 30 min. Final heating of the combination was place in an autoclave under static conditions for 24 hours at 150 °C; the resultant MCM-48 was then cooled down for 1 hour, filtrated, and rinsed with distilled H_2O before being dry at ambient temperature. The produced sample was then calcined for 6 hours at a temperature of 650 ºC applying a ramp rate for heating 2 °C/min.

2.3. Characterization

The MiniFlex (Rigaku) diffractometer was used to record the patterns of small-angle XRD in ambient settings using Cu K radiation (λ = 1.5406Å). The X-ray tube was run at 40 kV and 30 mA, and the data were reported in the 2θ range of 0.5-8° with a 2 step size of 0.01 and a step time of 10s. The formulae $n\lambda = 2d\sin\theta$ and $\alpha_o = 2d100/\sqrt{3}$ were applied to determine the unit cell and d-spacing characteristics. The pore analyzer of a micrometrics ASAP 2020 was used to assess the adsorption and desorption of nitrogen using N_2 physisorption at -196 °C. All specimens were degassed in the degas adsorption analyzer port for 3 hours at 350 °C and vacuum ($p < 10^{-5}$ mbar). The BET method was used to calculate the specimens' BET-specific surface areas for the relative pressure range of 0.05 to 0.25. With the use of the Barrett-Joyner-Halenda (BJH) approach, which is based on thermodynamics, the distributions of pore size were specified from the isotherm desorption branch. The quantity of liquid N_2 adsorbed at P/P_0 = 0.995 was used to calculate the total pore volume. This information was obtained from the N_2 isotherm's adsorption branch. Through the use of the unit cell parameter(α_o) and pore size diameter, the pore walls thickness (t_W) was estimated (d_P). Using BET analysis (4V/A), the average mesopore sizes for the single specimens were calculated from the data of nitrogen sorption. SEM was carried out on a JEOL (JSM-5600 LV). EDAX is an analytical method that creates the adsorbent elemental analysis to determine the composition of chemicals when combined with SEM. Using a NICOLET 380 FT-IR spectrometer, the solid samples' infrared spectra were measured were in the 4000 to 400 cm^{-1} range at areas with 4 cm^{-1} resolutions in transmission mode at ambient temperature.

2.4. Experiments of batch adsorption

To assess 3-Nitroaniline isotherms of adsorption onto the adsorbents at 25 °C, batch adsorption tests were performed. By dissolving 0.2 g of 3-Nitroaniline in 1 litre of distilled water, stock solutions of 3-Nitroaniline were created. At 25 °C, experiments of batch adsorption were used to assess the 3-Nitroaniline adsorption over the adsorbents. Then, 10 concentrations (0-0.2 g/L) were used to create a calibration curve using a UV-Spectrometer (model HP 8453) calibrated to 25 °C. λmax was discovered to be 278 nm for 3-Nitroaniline. The calibration was necessary to compare final absorbance with beginning absorbance. In 100 mL conical flasks, 15 different concentrations of the aforementioned solutions were created, starting from 0.001 - 0.06 g/L. 100 mL of each was added to 0.01g MCM-48, which was then stirred in several positions at 150 rpm for an hour at room temperature (25 °C). This made it possible for the mesoporous substance MCM-48 to completely mix with the mixture. Following the adsorption procedure, equal quantities of the solutions were centrifuged for five minutes at 3500 rpm using a centrifuge (model Hermle Z 200 A). This allowed the zeolite to completely separate from the solution and enable analysis with a UV-spectrophotometer (TU1900) operating at a wavelength of 278 nm. According to the following equation, the (%R) of 3-Nitroaniline was calculated (Eq.1) [28]:

$$\%R=\frac{Co-Ce}{Co}\times 100\% \quad (1)$$

Using the following equation, the amount of adsorption (qe) was determined (Eq.2) [29]:

$$qe=\frac{V(Co-Ce)}{m} \quad (2)$$

Where, qe (mg / g) denotes the adsorption amount, V (L) is the 3-Nitroaniline solution volume, m (g) is the mass of the absorbent applied used in the experiments, C_0 (mg/L) and C_e (mg/L) are the initial and equilibrium concentration of 3-Nitroaniline, respectively [30].

2.5. Adsorbent's reuse

The regeneration was studied applying an exhausted MCM-48 adsorbent. Following the 3-Nitroaniline adsorption solutions onto MCM-48, the mixture was filtered, the discarded adsorbent material that had uptake 3-Nitroaniline was rinsed in a sizable amount of H_2O until no 3-Nitroaniline remained in solution, and then dried under vacuum conditions at 60 °C for the duration of an entire night. Several adsorption-desorption cycles were achieved in order to examine the MCM-48 material's resilience and potential for regeneration.

3. Results and Discussion

3.1. Synthesized materials characterization

The prepared MCM- 48 was subjected to SEM and EDAX characterization procedures. At a magnification of 1000, SEM pictures of this material are displayed in

Figure 1a. The peaks on the EDAX graph in Figure 1b show the components' average weight % values that C, O, and Si made up the zeolite. To get accurate average weight % for each of the components, EDAX graphs were created for a number of different locations on the SEM pictures.

As can be displayed in Figure 2a, the MCM-48 small angle XRD patterns before and after adsorption exhibit a strong mesostructured-descriptive diffraction peak at around 2θ of 0.9°. Furthermore, two further peaks, indexed as (2 1 1), and (2 2 0) were seen in the XRD patterns. Two reflection peaks at 2θ less than 3° and a string of sporadic weak peaks in the range 3.5°–5.5° are indexed to the Ia3d cubic structure. When compared to comparable peaks described in the literature, the peaks acquired in our investigation match those reported there quite well [31]. The outcomes shown in Table 1 illustrate how MCM-48 has a periodic ordered structure and very stable before and after adsorption.

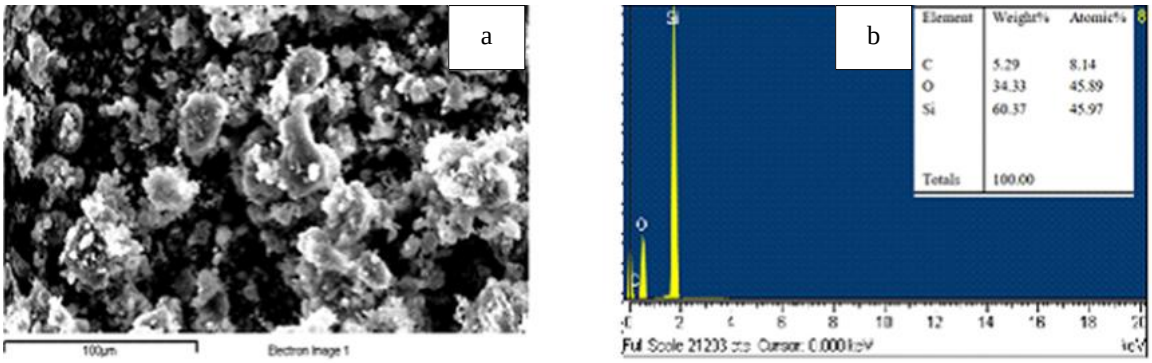

Figure 1: (a) SEM picture of MCM-48 at a 1000x magnification. (b) A typical MCM-48 EDAX picture.

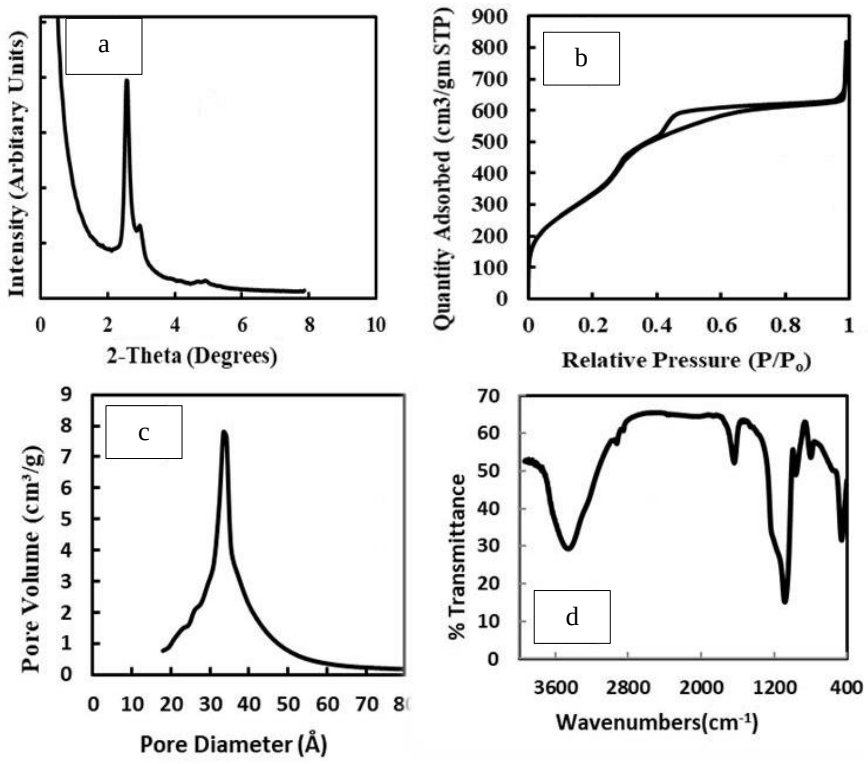

Figure 2: MCM-48 (a) X-ray diffraction pattern before and after adsorption (b) isotherms of nitrogen adsorption – desorption, (c) BJH pore size distribution, and (d) FT-IR spectra.

Table 1: MCM-48's physicochemical characteristics.

Sample	S_{BET} (m^2/g)	V_P (cm^3/g)	$V_{\mu P}$ (cm^3/g)	D_P (nm)	a_o (nm)	t_{wall} (nm)
MCM-48	1450	1.5	0.7	3.4	3.7	0.5

According to Figure 2b, the N_2 adsorption isotherms of MCM-48 have a type IV isotherm and a type H1 hysteresis loop. A small pore size distribution is indicated by sharp adsorption and desorption branches. The sharpness and height of the capillary condensation process in the isotherms, in general, represent the uniformity of the pore size for mesoporous molecular sieves. In the relative pressure (P/P_0) range of 0.05 to 0.25, the MCM-48 displays type IV isotherm, as illustrated in Figure 2b. Together with the structural features discovered by nitrogen adsorption investigations, Table 1 explains the sample's specific surface area, pore size, pore volume, and wall thickness together with the structural characteristics obtained from nitrogen adsorption studies.

Figure 2c displays the pore size distribution (PSD) for the MCM-48. The content produced by CTAB: NaOH: The pore size distribution of TEOS is broad and centered at 35 Å. A mesopores higher amount was discovered for the basic synthesization, which created the most evident pore size dispersion and had a fairly regular organization [32]. Figure 2d displays the FT-IR spectrum of MCM-48, which includes the characteristic Si-O-Si bands at 1082, 964,799, and 460 cm^{-1}. Stretching vibrations either Si OH or Si O Si can be attributed to the absorption band at around 960 cm^{-1}. Because of the existence of the surface OH groups and the strong H_2 bonding interactions between them, the wide band at approximately 3463 cm^{-1} is caused. Finally, the band at about 1637 cm^{-1} can be attributed to the distortion modes of the OH bonds of adsorbed H_2O [33].

3.2. 2-Nitroaniline adsorption

3.2.1. Contact time effect

The contact time duration was determined for the 3-Nitroaniline solution to adsorb it onto MCM-48 in order to attain equilibrium as indicated in Figure 3. λmax was discovered to be 278 nm for 3-Nitroaniline. The adsorption of 3-Nitroaniline solutions is clearly much influenced by time. The amount adsorbed on the nanoporous material zeolite was quantified for this purpose. The findings showed that equilibrium was established in under 20 minutes. It may take less time to attain balance. As a result, 60 minutes was specified to be the ideal contact time for the adsorbent. So, for the MCM-48 adsorbent to get saturated with analysis, just a very little contact time is needed. The adsorption capacity was greatly increased by higher cationic surfactant concentrations and their high availability in the pores of the adsorbent. This finding is significant, since one of the key factors taken into account for an efficient system of wastewater treatment is the equilibrium time. Therefore, in all experiments, adsorption was let to continue for 1 hour [34].

3.2.3. Effect of agitation rotary speed

The adsorption of hazardous solutes was examined by changing the agitation rotary speed from 0 to 200 rpm while maintaining a concentrated solution and contact time constant. The removal of harmful 3-Nitroaniline solutions rose when the agitation rotary speed was raised from 0 to 150 rpm; however, it then remained constant. This suggests that an agitation rotary speed in the 150-200 rpm range is enough to ensure the surfactants optimum cationic sites present in the pores of MCM-48 adsorbent are rapidly made available for absorption. The best agitation rotary speed for the remaining studies was determined to be 150 rpm [35].

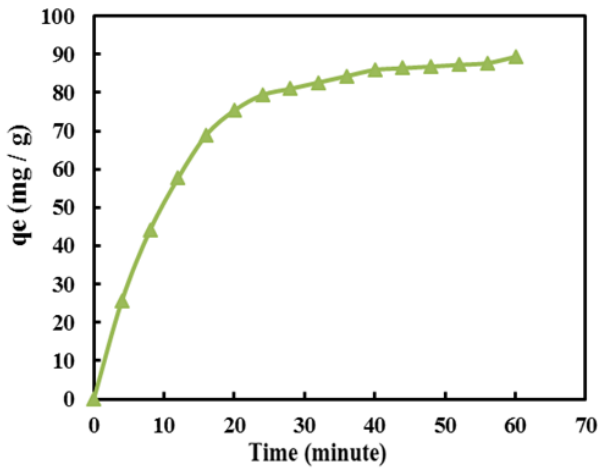

Figure 3: Contact time effect on the 3-Nitroaniline adsorption.

3.2.4. Concentration effect

As a 2-Nitroaniline initial concentration function C_0, Figure 4 depicts the % removal of 3-Nitroaniline estimated from Eq. 1. Approximately 64% of the 3-Nitroaniline content, which was initially 4 mg dm^{-3}, is removed from solution. The % removal of 3-Nitroaniline was decreased with the increased concentration at a constant mass of MCM-48. This reduces the amount of concentrated solution material that gradually absorbs more material. The quantity that may adsorb into the pores decreases when the maximum absorption of the MCM-48 pores is approached [36].

3.4 Adsorption isotherm

Figure 5 depicts the 3-Nitroaniline compound's adsorption isotherms, where Ce represents the adsorbate equilibrium concentration in solution at equilibrium and qe represents the adsorbate adsorbed per gram of MCM-48. 3-Nitroaniline molecule was generally adsorbed throughout a variety of concentrations, demonstrating the efficiency of MCM-48 in the removal of 3-Nitroaniline from aqueous solutions as an adsorbent. An essential driving factor for overcoming all ion and molecule mass transfer resistances between the solid phases and aqueous is the initial adsorbate concentration [37]. The initial solution concentration in the current investigation is adjusted from 4 - 60 mg/L however, the adsorbent dose stays constant at 0.01 g/100 mL. Figure 5 shows that when the equilibrium adsorption capacity increases, the initial 3-Nitroaniline concentration also rises.

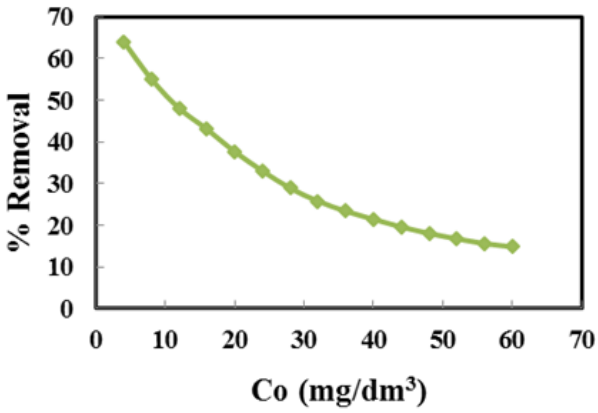

Figure 4: Initial 3-Nitroaniline concentration impact on removal efficiency at contact time=60 min and MCM-48 dosage=0.01 g.

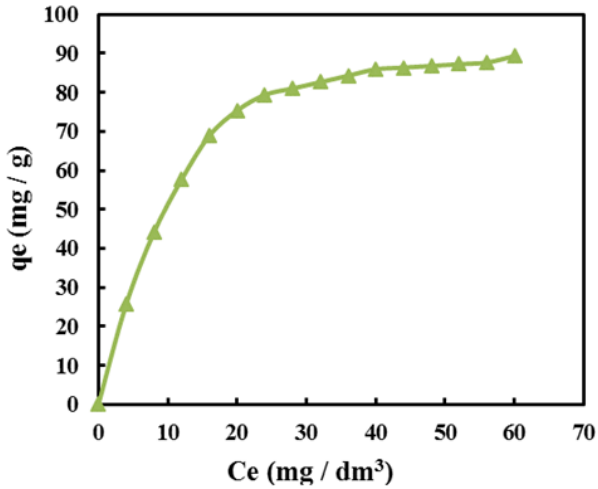

Figure 5: Isotherms of adsorption onto MCM-48 with 0.01g/100 mL adsorbent.

The uptake of equilibrium adsorption for 3-Nitroaniline rose from 20-89 mg/g as the starting concentration solution of 3-Nitroaniline was increased from 4 to 60 mg/L. This is because of the excess in number of 3-Nitroaniline molecules of poisonous solutes vying for the few remaining sites of binding onto the adsorbent's surface. According to the finding shown in Figure 5, cationic surfactants that include MCM-48 have a very high uptake for 3-Nitroaniline adsorption. As seen in Figure 2d, silanol groups (Si-OH) constitute significant sites of adsorption on the MCM-48surface. These sites are present in this substance in addition to cationic sites that were provided by a cationic template. It appears that a key determinant in the adsorption of 3-Nitroaniline on the surface of MCM-48 is the number of sorption sites. This can be explained by the fact that there are initially lots of empty surface sites accessible for adsorption. It was also proposed that as time went on, a potent attraction force developed between the molecules of 3-Nitroaniline and the sorbent. Due to saturation, it is difficult to fill the remaining open surface sites, which may also be related to a lack of accessible sorption sites towards the conclusion of the adsorption process [38].

The adsorption isotherms for 3-Nitroaniline compound have profiles that are consistent with Type I Langmuir adsorption; the quantity adsorbed rose gradually until it reached values in the 25-89 mg g^{-1} range [39]. The study of adsorption isotherms has been done so as to model the adsorption behavior.

According to Figures 6a and b, the Freundlich and Langmuir isotherm models were used to assess the 3-Nitroaniline species adsorption process. Equations of Langmuir and Freundlich are given in equations 3 and 4, respectively.

$$\frac{Ce}{qe} = \left(\frac{1}{bqmax}\right) + \left(\frac{1}{qmax}\right) Ce \quad (3)$$

$$\text{Log qe} = \text{Log KF} + \left(\frac{1}{n}\right) \text{Log Ce} \quad (4)$$

Graphing the Eq. 3 linear form of, or Ce/qe vs. Ce, which was applied to determine the constants of Langmuir and maximal uptake or capacity qmax, corroborated type I adsorption. According to Table 2 and Figure 9a, the Langmuir profile for the 3-Nitroaniline molecule is a straight line, supporting Type I adsorption. R^2 values are 0.99. Figure 6 displays the linearized isotherm data using the Langmuir equation. Table 2 lists the regression coefficients. R^2=0.99, a high correlation coefficient, denotes strong agreement between the parameters. 3-Nitroaniline has an adsorption ability to create monolayers that may reach up to 100 mg/g, according to the constant qmax. The value of the adsorption energy constant, b, for 3-Nitroaniline is 0.5 dm^3/mg. The Freundlich equation was also fitted to the similar data, which is seen in Figure 6b. Table 2 provides the constants of regression. The correlation coefficient values demonstrate how closely the data follow the Langmuir equation. The 3-Nitroaniline component adsorption on mesoporous materials is better depicted by the Langmuir model than by the Freundlich model. Furthermore, 3-Nitroaniline has 1/n values that are smaller than 1, which is a sign of a high adsorption intensity [40].

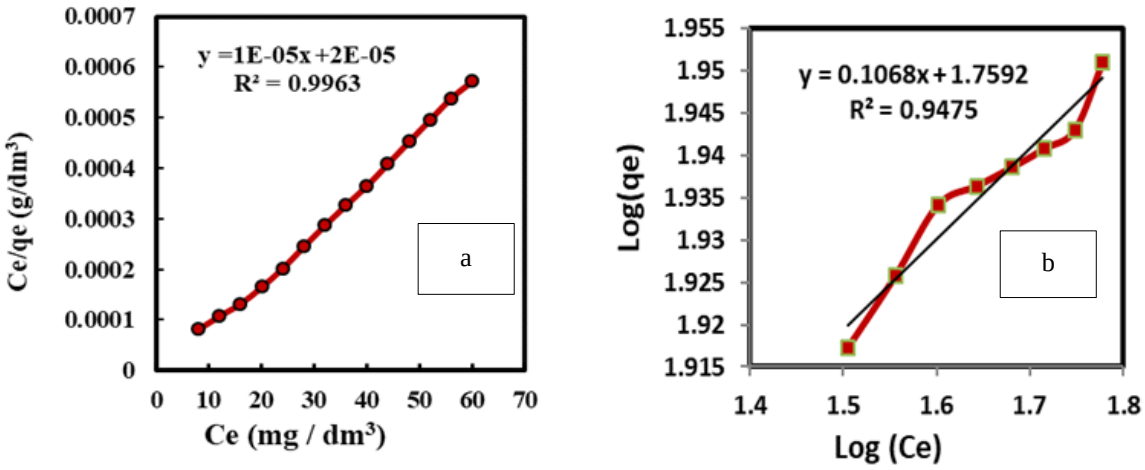

Figure 6: 3-Nitroaniline adsorption on MCM-48 according to (a) Langmuir, and (b) Freundlich isotherms.

Table 2: Constant of Langmuir and Freundlich for 3-Nitroaniline adsorption on MCM-48.

Adsorb ate	Langmuir constants				Freundlich constants	
	qmax ($mg.g^{-1}$)	b ($dm^3.mg^{-1}$)	R^2	K_F	1/n	R^2
3-nitroaniline	100	0.5	0.9963	57.438	0.1068	0.9475

3.5. Adsorption kinetics

One of the most important elements that defines the effectiveness of adsorption is the rate of 3-Nitroaniline adsorption by MCM-48. A pseudo-first and second order model have been applied to explain kinetics of 3-Nitroaniline adsorption. Figures 7a and b illustrate how pseudo-first- and second-order kinetics models were used to analyze the 3-Nitroaniline kinetics of adsorption onto MCM-48. Table 3 contains the results for the kinetic model parameters and the correlation coefficients (R^2). According to Table 3, the theoretical values (qe cal.) calculated from the pseudo-first-order kinetic model gave substantially different values when compared to experimental values (qe exp.). As a result, the pseudo 1st order kinetic model is representing this adsorption system well. The theoretical (qe cal.) and the experimental values (qe exp.) were calculated using the pseudo 2nd order kinetic model are extremely close to each other, as shown in Table 3. The coefficients R^2 value is also quite near to 1, which supports the validity of the pseudo-second-order equation. In the current research, the adsorption data were analyzed applying two important kinetic models. The integrated pseudo-first-order rate equation is written as [41]:

$$\text{Log}\,(qe-qt)=\text{Log}qe-k_1 t \quad (5)$$

The adsorbed 3-Nitroaniline quantity at equilibrium time t is shown by qe and qt, respectively. k_1 : is the pseudo-first-order adsorption equilibrium rate constant. The pseudo-second-order equation is [42]:

$$\frac{t}{qt}=\frac{1}{k_2 qe^2}+\frac{1}{qe}t \quad (6)$$

k_2: is the rate constant of pseudo-second-order.

Figures 7a and b explain the findings of Pseudo-first and second order models were used to fit the experimental data, respectively. The results from the adsorption kinetics are extremely well matched by the pseudo-second order model, as shown in Figure 7b. Given that 3-Nitroaniline regression coefficients are so high (0.99), the pseudo 2nd order hypothesis for the adsorption mechanism process appears to be well-supported [43].

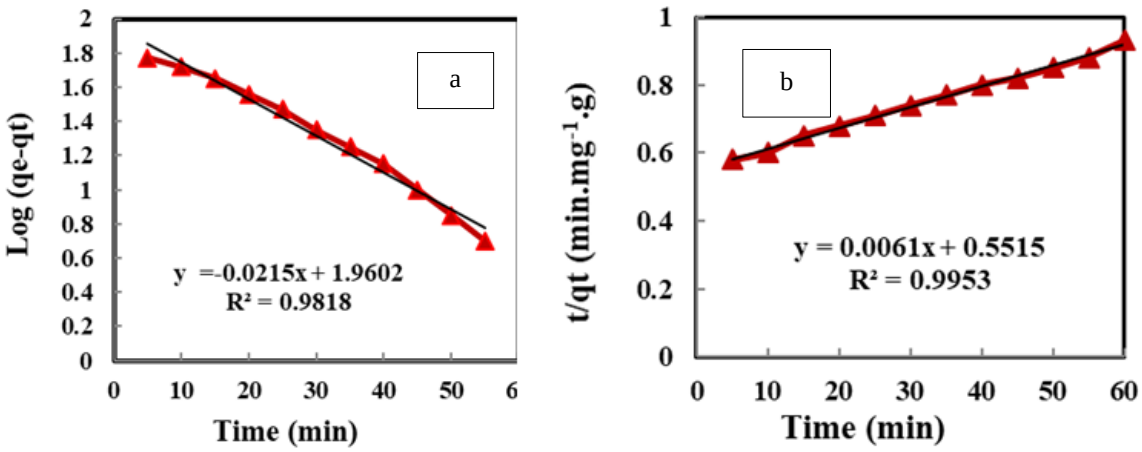

Figure7: (a) Pseudo 1st and (b) 2nd order kinetics for the 3-Nitroaniline adsorption on MCM-48.

Table 3: Kinetics parameters values for 3-Nitroaniline adsorption on MCM-48.

Adsorbates	qe.exp. (mg/g)	Pseudo-first order constants			Pseudo-second order constants		
		qe.cal. (mg/g)	K_1 (g/mg.min)	R^2	qe.cal. (mg/g)	K_2 (g/mg.min)	R^2
3-Nitroaniline	65	91	0.0215	0.981	163	$6.747*10^{-5}$	0.995

3.6. Adsorption thermodynamics

As shown in Figure 8, the thermodynamic parameters for the adsorption of 3-Nitroaniline at different temperatures are given in Table 4 by the plot of the linear Van't Hoff equation (ln kc versus 1/T). The negative values of ΔG for applied temperatures are a sign of spontaneous sorption. Besides, the value of ΔS was negative, demonstrating that the adsorption process could reduce chaos degree of the system, Furthermore, the value of ΔS was negative, showing that the sorption process reduced chaos. while the negative value of enthalpy ΔH indicates that the sorption is exothermic.

3.7. Adsorption mechanism

To understand the adsorption mechanism process, it is important to know the structure of the adsorbent and adsorbate as shown in Figure 9 3-Nitroaniline molecule is an organic chemical substance, particularly a primary aromatic amine. It consists of an amino group attached to a benzene ring. On the other hand, MCM-48 adsorbent is the most common molecular sieves of mesoporous materials that is intensively investigated by researchers. The most notable feature of the MCM-48 is that despite having an amorphous silica wall, it has a long-range organized structure and consistent mesoporous. This important material has the majority of silanol group. Based on the structure of the 3-Nitroaniline, MCM-48 and experimental results of kinetic, FTIR and EDX analysis, the adsorption mechanism of 3-Nitroaniline onto MCM-48 adsorbent can be determined. Based on FTIR results, the strong adsorption band of at – C = C–group was decreased in intensity and shifted from 1681 to 1600 cm^{-1} owing to π–π interactions between 3-Nitroaniline molecule with – C = C– onto the surface of MCM-48. While the band of – OH groups was increased in intensity and a slight shift from 3330 to 3335 owing to hydrogen bond formation between the $–N(CH_3)_2$ group of 3-Nitroaniline molecules and the – OH group in the MCM-48 surface. The band of C = O stretch vibration of carboxylic acid was a slight increase in intensity due to electrostatic attraction between a cationic $^{+}N(CH_3)_3^{+}$ group of MG molecules with the negative charge of COOH group onto the MCM-48 surface. According to the results of adsorption isotherms and kinetics study, the adsorption mechanism is a chemisorption and physical adsorption process. Therefore, these results provide enough evidence to support the 3-Nitroaniline adsorption onto the MCM-48 surface by different mechanisms such as hydrogen bonding, electrostatic interaction and π-π interactions [44, 45].

Table 4: Thermodynamic parameters for the sorption 3-Nitroaniline on MCM-48 at different temperatures.

Adsorbent	T/^{0}K	Kc L/ g	ΔG kJ/mol	ΔH kJ/mol	ΔS J /mol. k	R^2
MCM-48	298	11.11	-5.83	-23.84	-60.21	0.9721
	308	7.44	-5.03			
	318	6.07	-4.66			

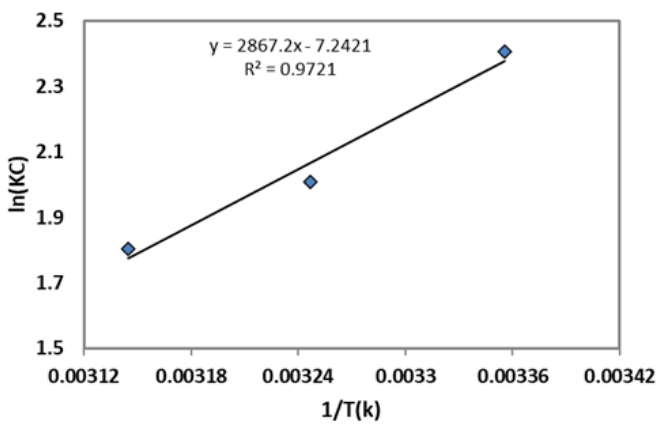

Figure 8: Plot of ln Kc versus 1/T for 3-Nitroaniline sorption by 0.01g of MCM-48 (C_o=10, time=60 min, RPM=150).

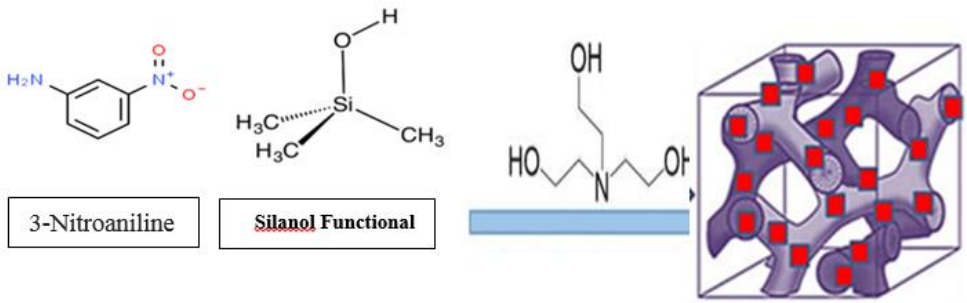

Figure 9: Mechanism adsorption of 3-Nitroaniline onto MCM-48 adsorbent.

3.8. Adsorbent reuse

The possibility of recycling the adsorbent was examined for applying a depleted MCM-48 after regeneration. For the purpose of proving that the MCM-48 could be regenerate by removing the adsorbates, desorption investigations were carried out. When using the MCM-48 again, it is crucial to establish that desorption takes place. According to the results of the trials, 3-Nitroaniline was effectively and efficiently desorbed into deionized water in a single cycle, with an efficiency of over 90 %. It can be seen from this that used materials may be recycled. It is possible to perform a more thorough investigation to learn more about desorption, including the impacts of solution concentration, adsorbate loading, temperature, etc. The focus of this essay does not extend to this study [46].

4. Conclusion

In this study, 3-Nitroaniline was easily adsorbed from an aqueous adsorbate solution utilizing from the MCM-48 mesoporous material. According to a linear analysis with R^2 values of 0.99, 3-Nitroaniline molecules matched to Type I Langmuir adsorption. Under appropriate experimental circumstances, nanoporous material demonstrated considerable aniline adsorption capacity; as a result, it may be suggested as a practical adsorbent. The Langmuir adsorption isotherm was discovered the best suited with the experimental, indicating monolayer adsorption on a homogeneous surface. The Langmuir isotherm was used to calculate the theoretical and experimental maximal adsorption capacity of 100 mg g^{-1}, and 89 mg g^{-1}, respectively. The pseudo-second-order model can forecast the dynamics of adsorption. Adsorption isotherms and kinetics models indicate that chemical and physical adsorption are the two processes involved in the adsorption mechanism. It is obvious from the negative Gibbs free energy change of the adsorption that it is a spontaneous adsorption. Adsorption is an exothermic process as indicated by the negative enthalpy change. At equilibrium, 3-Nitroaniline adsorption decreases with increasing temperature.

Acknowledgments

The authors are grateful to the Department of Chemical Engineering at the University of Technology-Iraq, the Mustansiriyah University/ College of Engineering/ Materials Engineering Department Baghdad-Iraq, the Department of Chemical and Petroleum Industries Engineering, Al-Mustaqbal University College.

5. References

1. A. Al-Nayili, H. Sh. Majdi, T. M. Albayati, N. M. Cata Saady., Formic acid dehydrogenation using noble-metal nanoheterogeneous catalysts: towards sustainable hydrogen-based energy, *Catal.* 12(2022), 324-336.
2. S. M. Alardhi, J. M. Alrubaye, T. M. Albayati, Removal of methyl green dye from simulated waste water using hollow fiber ultrafiltration membrane, 2nd International Scientific Conference of Al-Ayen University (ISCAU-2020).
3. J. O'Brien, T.F. O'Dwyer, T. Curtin, A novel process for the removal of aniline from wastewaters, *J. Hazard. Mater.*, 159(2008), 476-482.
4. M. Sadeghi-Kiakhani, E. Hashemi, Study on the effect of pomegranate peel and walnut green husk extracts on the antibacterial and dyeing properties of wool yarn

treated by chitosan/Ag, chitosan/Cu nano-particles, *Prog. Color Colorants Coat.*, 16(2023), 221-229.

5. C. Ko, S. Chen, Enhanced removal of three phenols by lactase polymerization with MF/UF membranes, *Bioresour. Technol.*, 99(2008), 2293-2298.
6. N. S. Ali, K. R. Kalash, A. N. Ahmed & T. M. Albayati, Performance of a solar photocatalysis reactor as pretreatment for wastewater via UV, UV/TiO_2, and UV/H_2O_2 to control membrane fouling, *Sci. Rep.*, 12(2022), 16782.
7. N.S. Abbood, N.S. Ali, E.H. Khader, H.Sh. Majdi, T.M. Albayati, N.M. Cata Saady, Photocatalytic degradation of cefotaxime pharmaceutical compounds onto a modified nanocatalyst, *Res. Chem. Intermed.*, 49(2023), 43-56.
8. A.L. Ahmad, K. Y. Tan, Reverse osmosis of binary organic solute mixtures in the presence of strong solute-membrane affinity, *Desalin*, 165(2004), 193-199.
9. V.V. Goncharuk, D.D. Kucheruk, V.M. Kochkodan, V.P. Badekha, Removal of organic substances fromaqueous solutions by reagent enhanced reverse osmosis, *Desalin*, 143(2002), 45-51.
10. T. Hirakawa, T. Daimon, M. Kitazawa, N. Ohguri, C. Koga, N. Negishi, S. Matsuzawa, Y. Nosaka. An approach to estimating photocatalytic activity of TiO_2 suspension by monitoring dissolved oxygen and superoxide ion on decomposing organic compounds, *J. Photochem. Photobiol.*, 190(2007), 58-68.
11. A. M. Amat, A. Arques, M. A. Miranda, S. Segu´ı, R.F. Vercher, Degradation of rosolicacid by advanced oxidation processes: ozonation vs. solar photocatalysis, *Desalin*, 212(2007), 114-122.
12. G. L. Puma, P. L. Yue, Effect of the radiation wavelength on the rate of photocatalyticoxidation of organic pollutants, *Ind. Eng. Chem. Res.*, 41(2002), 5594-5600.
13. B. M. Nader, Performance of advanced methods for treatment of wastewater: UV/TiO_2, RO and UF, *Chem. Eng. Process.*, 43(2004), 935-940.
14. R. Morent, J. Dewulf, N. Steenhaut, C. Leys, H. Van Lagenhove, Hybrid plasmacatalyst system for the removal of trichloroethylene from air, *J. Adv. Oxid. Technol.*, 9(2006), 53-58.
15. J. Levec, A. Pintar, Catalytic wet-air oxidation processes: a review, *Catal. Today*, 124(2007), 172-184.
16. S.K. Bhargava, J. Tardio, H. Jani, D.D. Akolekar, K. Foeger, M. Hoang, Catalytic wet-air oxidation of industrialwaste streams, *Catal. Surv. Asia*, 11(2007), 70-86.
17. C. H. Ko, C. Fan, P. N. Chiang, M. K. Wang, K. C. Lin, *p*-Nitrophenol, phenol and aniline sorption by organo-clays, *J. Hazard. Mater.*, 149(2007), 275-282.
18. S. Razee, T. Masujima, Uptake monitoring of anilines and phenols using modified zeolites, *Anal. Chim. Acta.*, 464(2002), 1-5.
19. N. A. Atiyah, T. M. Albayati, M. A. Atiya, Functionalization of mesoporous MCM-41 for the delivery of curcumin as an anti-inflammatory therapy, *Adv. Powder Technol.*, 33(2022), 103417.
20. N. A. Atiyah, T. M. Albayati, M. A. Atiya., Interaction behavior of curcumin encapsulated onto functionalized SBA-15 as an efficient carrier and release in drug delivery, *J. Mol. Struct.*, 1260(2022), 132879.
21. E. Narita, N. Horiguchi, T. Okabe, Adsorption of phenols, cresols and benzyl alcohol from aqueous solution by silicalite, *Chem. Lett.*, 6(1985), 787-790.
22. U. S. Taralkar, M. W. Kasture, P .N. Joshi, Influence of synthesis condition on structure properties of MCM-48, *J. Phys. Chem. Sol.*, 69(2008), 2075-2081.
23. L. Pajchel, W. Kolodziejski. Synthesis and characterization of MCM 48/hydroxyapatite composites for drug delivery: Ibuprofen incorporation, location and release studies, *Mater. Sci. Eng. C*, 91(2018), 734-742.
24. M. Shaban, M. R. Abukhadra, A. Hamd, R. R. Amin, A. A. Khalek. Photocatalytic removal of Congo red dye using MCM-48/Ni_2O_3 composite synthesized based on silica gel extracted from rice husk ash; fabrication and application, *J. Environ. Manage.*, 204(2017), 189-199.
25. R. Nejat, A. R. Mahjoub, Z. Hekmatian, A. Tahereh. Pd-functionalized MCM-41 nanoporous silica as an efficient and reusable catalyst for promoting organic reactions, *RSC Adv.*, 5(2015), 16029-16035.
26. A. M. Doyle, B. K. Hodnett, Synthesis of 2-cyanoethyl-modified MCM-48 stable to surfactant removal by solvent extraction: Influence of organic modifier, base and surfactant, *Micropor, Mesopor. Mater.*, 58(2003), 255-261.
27. A. M. Doyle, E. Ahmed, B. K. Hodnett, The evolution of phases during the synthesis of the organically modified catalyst support MCM-48, *Catal. Today*, 116(2006), 50-55.
28. N. S. Ali, N. M. Jabbar, S. M. Alardhi, H. Sh. Majdi, T. M. Albayati, Adsorption of methyl violet dye onto a prepared bio-adsorbent from date seeds: isotherm, kinetics, and thermodynamic studies, *Heliyon*, 8(2022), e10276,
29. W. A. Muslim, T. M. Albayati, S. K. Al-Nasri, Decontamination of actual radioactive wastewater containing ^{137}Cs using bentonite as a natural adsorbent: equilibrium, kinetics, and thermodynamic studies, *Sci. Rep.*, 12(2022), 13837.
30. Y. A. Abd Al-Khodor, T. M. Albayati, Real heavy crude oil desulfurization onto nanoporous activated carbon implementing batch adsorption process: equilibrium, kinetics, and thermodynamic studies, *Chem. Afr.*, 6(2023), 747-756
31. S. Han, J. Xu, W. Hou, X. Yu, and Y. Wang, Synthesis of high-quality MCM-48 mesoporous silica using Gemini surfactant dimethylene- 1,2-bis (dodecyldimethylammonium bromide), *J. Phys. Chem. B*, 108(2004), 15043-15048.
32. Z. Qiang, X. Bao, W. Ben, MCM-48 modified magnetic mesoporousnanocomposite as an attractive

adsorbent for the removal of sulfamethazine from water, *Water Res.*, 47(2013), 4107-4114.
33. T. M. Al-Bayati, Removal of aniline and nitro-substituted aniline from wastewater by particulate nanoporous MCM-48, *Part. Sci. Technol.*, 32(2014), 616-623.
34. H. Tian, J. Li, L. Zou, Z. Mua and Z. Hao, Removal of DDT from aqueous solutions using mesoporous silica materials, *J. Chem. Technol. Biotechnol.* 84(2009), 490-496.
35. T. M. Albayati, A. M. Doyle. Purification of aniline and nitrossubistituted aniline contaminants from aqueous solution using beta zeolite, *Chem. Bulgarian J. Sci. Edu.*, 23(2014), 105-114.
36. S. Fauzia, H. Aziz, D. Dahlan, R. Zein. Study of equilibrium, kinetic and thermodynamic for removal of Pb(II) in aqueous solution using Sago bark (Metroxylon sago), AIP Conference Proceedings 2023, 020081 (2018).
37. T. M. Albayati, A. M. Doyle., Shape-selective adsorption of substituted aniline pollutants from wastewater, *Adsorpt. Sci. Technol.*, 31(2013), 459-468.
38. T. M. Albayati, A. A. Sabri, D. B. Abed, Adsorption of binary and multi heavy metals ions from aqueous solution by amine functionalized SBA-15 mesoporous adsorbent in a batch system, *Desalin. Water Treat.*, 151(2019), 315-321.
39. R. Saad, K. Belkacemi, S. Hamoudi, Adsorption of phosphate and nitrate anions on ammonium-functionalized MCM-48: effects of experimental conditions, *J. Colloid Interface. Sci*., 311(2007), 375-381.
40. A. T. Khadim, T. M. Albayati, N. M. Cata Saady, Desulfurization of actual diesel fuel onto modified mesoporous material Co/MCM-41, *Environ. Nanotechnol. Monit. Manag.*, 17(2022), 100635.
41. S. T. Kadhum, G. Y. Alkindi, T. M. Albayati, Remediation of phenolic wastewater implementing nano zerovalent iron as a granular third electrode in an electrochemical reactor, *Int. J. Environ. Sci. Technol*., 19(2022), 1383-1392.
42. S. T. Kadhum, G. Y. Alkindi, T. M. Albayati, Determination of chemical oxygen demand for phenolic compounds from oil refinery wastewater implementing different methods, *Desalin. Water Treat.*, 231(2021), 44-53.
43. E. H. Khader, R. H. Khudhur, N. S. Abbood, T. M. Albayati, Decolourisation of anionic azo dye in industrial wastewater using adsorption process: investigating operating parameters, *Environ. Process.*, (2023), DOI: 10.1007/s40710-023-00646-7.
44. A. Amari, H.S.K. Alawamleh, M. Isam, M. A. J. Maktoof, H. Osman, B. Panneerselvam, M. Thomas, Thermodynamic investigation and study of kinetics and mass transfer mechanisms of oily wastewater adsorption on UIO-66–$MnFe_2O_4$ as a metal–organic framework (MOF), *Sustain*., 15(2023), 2488.
45. A. Q. Alorabi, M. Azizi, Effective removal of methyl green from aqueous environment using activated residual Dodonaea Viscosa: equilibrium, isotherm, and mechanism studies, *Environ. Pollut. Bioavailab.*, 35(2023), 2168761.
46. H. J. Al-Jaaf, N. S. Ali, S. M. Alardhi, T. M. Albayati, Implementing eggplant peels as an efficient bio-adsorbent for treatment of oily domestic wastewater, *Desalin. Water Treat.*, 245(2022), 226-237.

How to cite this article:
A. E. Mahdi, N. S. Ali, K. R. Kalash, I. K. Salih, M. A. Abdulrahman, T. M. Albayati, Investigation of Equilibrium, Isotherm, and Mechanism for the Efficient Removal of 3-Nitroaniline Dye from Wastewater Using Mesoporous Material MCM-48. Prog. Color Colorants Coat., 16 (2023), 387-398.